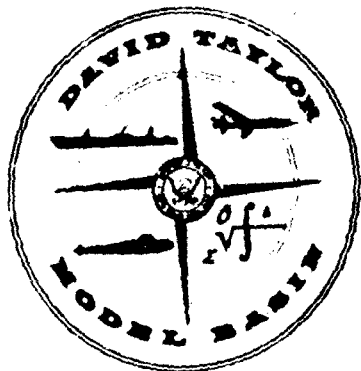


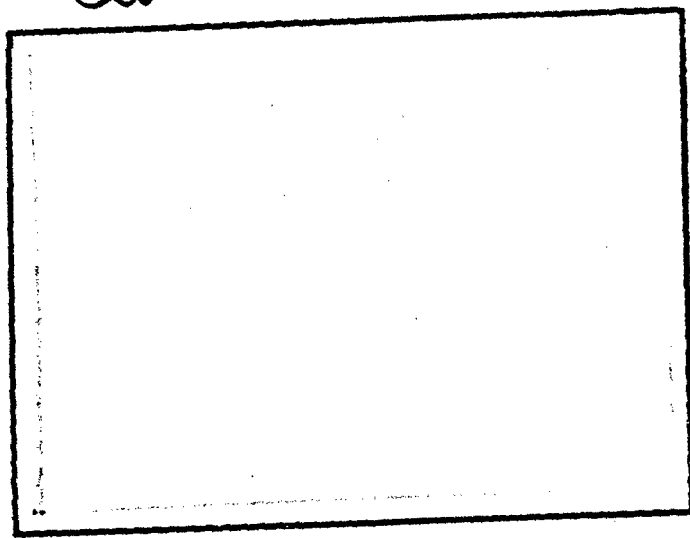
HML NO.
001027 173-H-01

ADA 071 772



MOST Project-4 **LEVEL**
TEST REPORT

0000073/232



DDC FILE COPY

001027
8/215

PRNC-TNS-936

DDC
JUL 27 1979
A

HYDROMECHANICS LABORATORY
DAVID TAYLOR MODEL BASIN
DEPARTMENT OF THE NAVY
WASHINGTON, D.C.

Approved for public release
Distribution unlimited

Reproduced From
Best Available Copy

9/12/1966

14
HNL-
Report 173-H-01

11
August 1966

6
DRAG CHARACTERISTICS OF A
SYSTEMATIC SERIES OF TRAILING-
TYPE CABLE FAIRINGS
(DTMB SERIES B)

12
30p. DDC
JUL 27 1979
REUNITED
A

10
by
James P. Ramsey and Thomas Gibbons

DISTRIBUTION STATEMENT A
Approved for public release;
Distribution Unlimited

104670

118

DEPARTMENT OF THE NAVY
DAVID TAYLOR MODEL BASIN
WASHINGTON, D. C. 20374

EXACTLY REPLY TO
173
DTMB:SS

19 AUG 1966

From: Commanding Officer and Director, David Taylor Model Basin
To: Distribution List

Subj: David Taylor Model Basin Hydromechanics Laboratory Test
Report 173-II-01; forwarding of

Encl: (1) David Taylor Model Basin Hydromechanics Laboratory Test
Report 173-II-01, " Drag Characteristics of a Systematic
Series of Trailing-Type Cable Fairings (DTMB Series B),"
by James P. Ramsey and Thomas Gibbons

1. Enclosure (1) is forwarded herewith for your information and
retention.

J. B. Hadley
J. B. HADLEY
By direction

Distribution List

SHIPS 1622, 1633D, 6671, 6687C, 6687C1
AIR 53302
ONR (468)
SP (204)
ASL (9340)
NRL (5442)
MEL (683)
NEL
USN/USL (930)
SAS (ASW-926)
NAVMINDEFLAB
Defense Research Laboratory, University of Texas
Hydronautics, Inc. (Mr. P. Eisenberg)
Boeing Aircraft Co.
North American Aviation, Inc.
Hydrospace Research Corporation
Naval Research Establishment
McKiernan Terry, Marine Division of Litton Industries
EDO, Inc.
TRACOR, Inc.

LIST OF FIGURES

	Page
Figure 1 - Basic Configuration of the Series A Shape	3
Figure 2 - Sketch of Section Shapes of Series A Test Models	6
Figure 3 - Trailing Fairing Test Models	8
Figure 4 - Two-Dimensional Fairing Dynamometer	10
Figure 5 - Gage Arrangement	11
Figure 6 - Instrumentation Arrangement	12
Figure 7 - Typical Test Arrangement	13
Figure 8 - Drag Coefficient as a Function of Reynolds Number for a Thickness Ratio of 0.6	15
Figure 9 - Drag Coefficient as a Function of Reynolds Number for a Thickness Ratio of 0.8	16
Figure 10 - Drag Coefficient as a Function of Reynolds Number for a Thickness Ratio of 1.0	17
Figure 11 - Effect of Fineness Ratio on Drag Coefficient	18
Figure 12 - Effect of Fineness Ratio on Residual-Resistance Coefficient	19
Figure 13 - Effect of Thickness Ratio on Drag Coefficient.	20
Figure 14 - Effect of Thickness Ratio on Residual-Resistance Coefficient.	21

LIST OF TABLES

Table 1 - Geometrical Parameters of Series A and B Shapes	7
Table 2 - Physical Characteristics of Series B Models	9

NO. _____	
Date _____	✓
Time _____	
By _____	
<i>Letter on file</i>	
Distribution _____	
Availability Codes	
Dist. _____	Available/or Special
A	

NOTATION

A_f	Projected frontal area of cable fairing combination
c	Chord of fairing
C_D	Drag coefficient based on frontal area of cable, $C_D = \frac{D}{\frac{1}{2} \rho V^2 A_f}$
C_f	Frictional-resistance coefficient
C_r	Residual-resistance coefficient, $C_r = C_t - C_f$
C_t	Total-drag coefficient based on wetted surface, $C_t = \frac{D}{\frac{1}{2} \rho V^2 S}$
d	Diameter of cable
D	Total hydrodynamic drag
l	Characteristic length
R	Reynolds number, $R = \frac{Vl}{\nu}$
S	Total wetted surface area
t	Maximum thickness of fairing
V	Speed
ρ	Mass density of fluid
ν	Kinematic viscosity

INTRODUCTION

The David Taylor Model Basin is engaged in a broad research program to provide fundamental hydrodynamic data which can be applied to the design of improved cable-towed-body systems. Pursuant thereto, a number of years ago, the Model Basin originated a systematic series of trailing-type fairings (now designated Series A) and conducted an experimental program to investigate the effect of variations in geometric parameters on the hydrodynamic characteristics of such fairings¹⁻³. Subsequently, when selected shapes of Series A were applied in actual towing systems, certain difficulties associated with mechanical construction were encountered. To avoid similar problems in the future, Series A was revised to obtain a new series of trailing fairings designated as Series B. Nine models of the new series were assembled and drag experiments at zero angle of attack, the results of which form the subject of this report, were conducted in the towing basin.

This report derives the basic geometry of Series B, describes the models used for the tests, describes the special purpose dynamometer and other apparatus used in the test, outlines the test procedures, presents data curves for the individual models showing variation of drag coefficient with Reynolds number, and presents summary curves showing the variation of drag coefficient with the nondimensional geometric parameters (fineness ratio and thickness ratio). Conclusions are drawn concerning the selection of series shapes from the standpoint of minimizing drag of towables.

GEOMETRY OF SERIES

DTMB Series B is a systematic series of trailing-type fairings. The configuration of the parent form of the series is based on the concept of a clip-on fairing wherein the towable provides the leading edge of the fairing, as opposed to the enclosed type of fairing which completely houses the cable. The precise shape of the individual forms of the series

¹ References are listed on page 24.

is defined in terms of the prescribed geometrical parameters, fineness ratio $\frac{S}{d}$ and thickness ratio $\frac{t}{d}$. As mentioned in the Introduction, Series B was obtained by modifying Series A. The modification consisted essentially of the elimination of the gap between the fairing and the cable. The detailed derivation of the analytical expression for Series A (including the gap) has not been previously published. Consequently, to avoid confusion in identifying the various configurations, a detailed derivation is given in the following paragraphs.

The basic configuration of Series A is shown in Figure 1. The equation defining the shape is derived from a cubic of the form:

$$y = A_1 (x-x_0)^3 + A_2 (x-x_0)^2 + A_3 (x-x_0) + A_4 \quad [1]$$

where $(x-x_0)$ is the abscissa of the fairing shape in a coordinate system with the origin at the leading edge of the cable.

The constants A_1, A_2, A_3 , and A_4 can be evaluated as follows: when $x = x_0$, let $\frac{dy}{dx} = 0$ and $\frac{d^2y}{dx^2} = 0$, then

$$\frac{dy}{dx} = 3A_1 (x-x_0)^2 + 2A_2 (x-x_0) + A_3 = 0 \quad [2]$$

and

$$\frac{d^2y}{dx^2} = 6A_1 (x-x_0) + 2A_2 = 0. \quad [3]$$

Thus A_2 and $A_3 = 0$.

Equation [1] becomes

$$y = A_1 (x-x_0)^3 + A_4. \quad [4]$$

Now let $y = 0.5t$ at $x = x_0$, so that

$$A_4 = 0.5t.$$

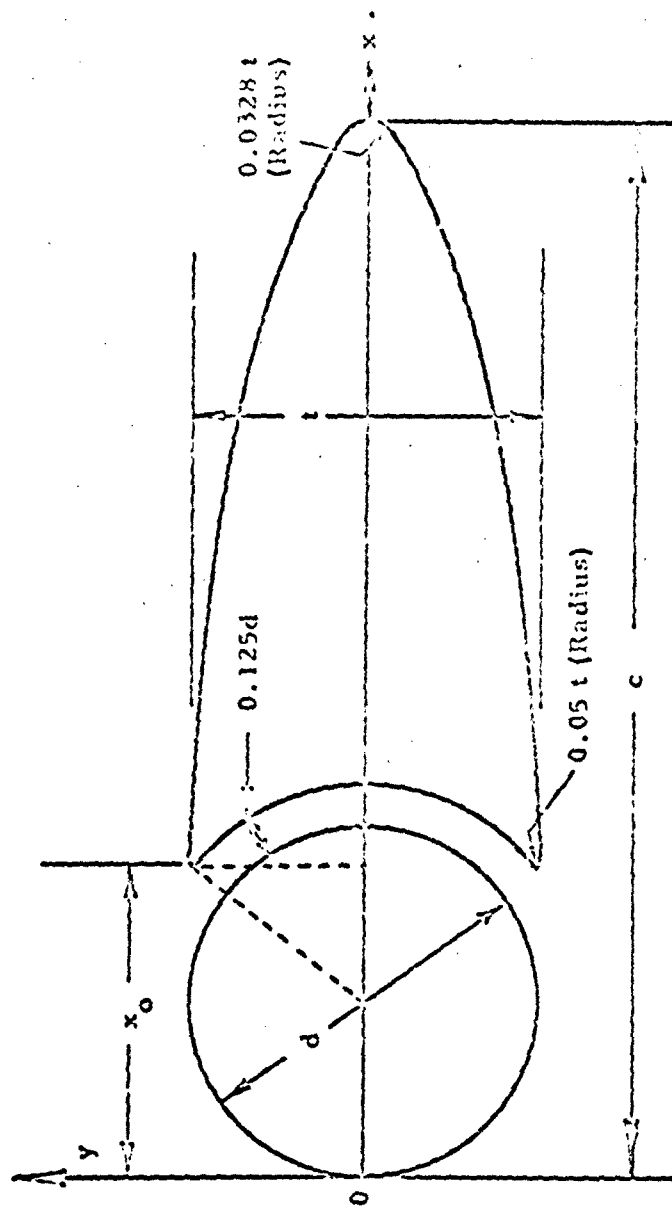


Figure 1 - Basic Configuration of the Series A Shape

Equation [4] can now be written as

$$y = A_1 (x - x_0)^n + 0.5t. \quad [5]$$

Due to manufacturing considerations it is desirable to avoid a knife edge at the termination of the fairing. This is achieved by giving a value of y equal to 2.5 percent of t at $x = c$ and evaluating A_1 :

$$0.025t = A_1 (c - x_0)^n + 0.5t$$

and

$$A_1 = \frac{-0.475t}{(c - x_0)^n}.$$

All the constants have been determined and Equation [5] becomes

$$y = 0.5t - 0.475t \frac{(x - x_0)^n}{(c - x_0)^n} \quad [6]$$

which expressed in nondimensional form is

$$y/t = 0.5 - 0.475 \frac{(x - x_0)^n}{(c - x_0)^n}. \quad [7]$$

Let $y/t = y'$, $\frac{x}{c} = x'$ and $\frac{x_0}{c} = x_0'$.

Thus Equation [7] becomes

$$y' = 0.5 - 0.475 \frac{(x' - x_0')^n}{(1 - x_0')^n}. \quad [8]$$

As expressed by Equation [8], the fairing trailing edge terminates in a blunt end. To eliminate the blunt end, the fairing shape was terminated by the arc of a circle (found by graphical methods) with radius $r = 0.0328t$ which intersects the x axis at $x = c$ and is tangent to the curve which forms the fairing.

Referring to Figure 1, an expression for x_0 is found as follows:

$$(x_0 - 0.5d)^2 = (0.625d)^2 - (0.5t)^2 \quad [9]$$

$$x_0 - 0.5d = \sqrt{(0.625d)^2 - (0.5t)^2}$$

$$x_0 = 0.5d + \sqrt{(0.625d)^2 - (0.5t)^2}. \quad [10]$$

Equation [10] can be written in nondimensional form as

$$x_0' = \frac{x_0}{c} = \frac{0.5d}{c} + \sqrt{(0.625\frac{d}{c})^2 - (0.5\frac{t}{c})^2}. \quad [11]$$

Since $\frac{t}{c} = \frac{t}{d} \cdot \frac{d}{c}$,

Equation [11] assumes the final form

$$x_0' = \frac{d}{c} \left(0.5 + \sqrt{(0.625)^2 - (0.5\frac{t}{d})^2} \right). \quad [12]$$

Graphical methods were also employed to obtain the value of 0.05t for the radius of the circles which terminate the leading edge. It should be realized that Equations [8] and [12] apply only between the tangency point of the leading- and trailing-edge circles.

Figure 2 shows the configurations of the nine Series A models that were used in the wind-tunnel tests^{1,2,3}. These configurations were obtained from Equations [8] and [12] using thickness ratios $\frac{t}{d}$ of 0.6, 0.8, and 1.0 in combination with fineness ratios $\frac{c}{d}$ of 3, 4, and 5. The individual models of Series A are identified by the letters TF followed by a two digit number which denotes the fineness ratio and thickness ratio. Thus, Series A Model TF-84 is a trailing fairing having thickness ratio of 0.8 and fineness ratio of 4.0. Model TF-15 is trailing fairing with thickness ratio of 1.0 and fineness ratio of 5.0.

Since the gap between the cable and fairing is eliminated, the comparable shapes of Series B have the same thickness ratios as those of Series A but somewhat different fineness ratios. Table 1 compares geometrical parameters of Series A and B shapes that have been tested.

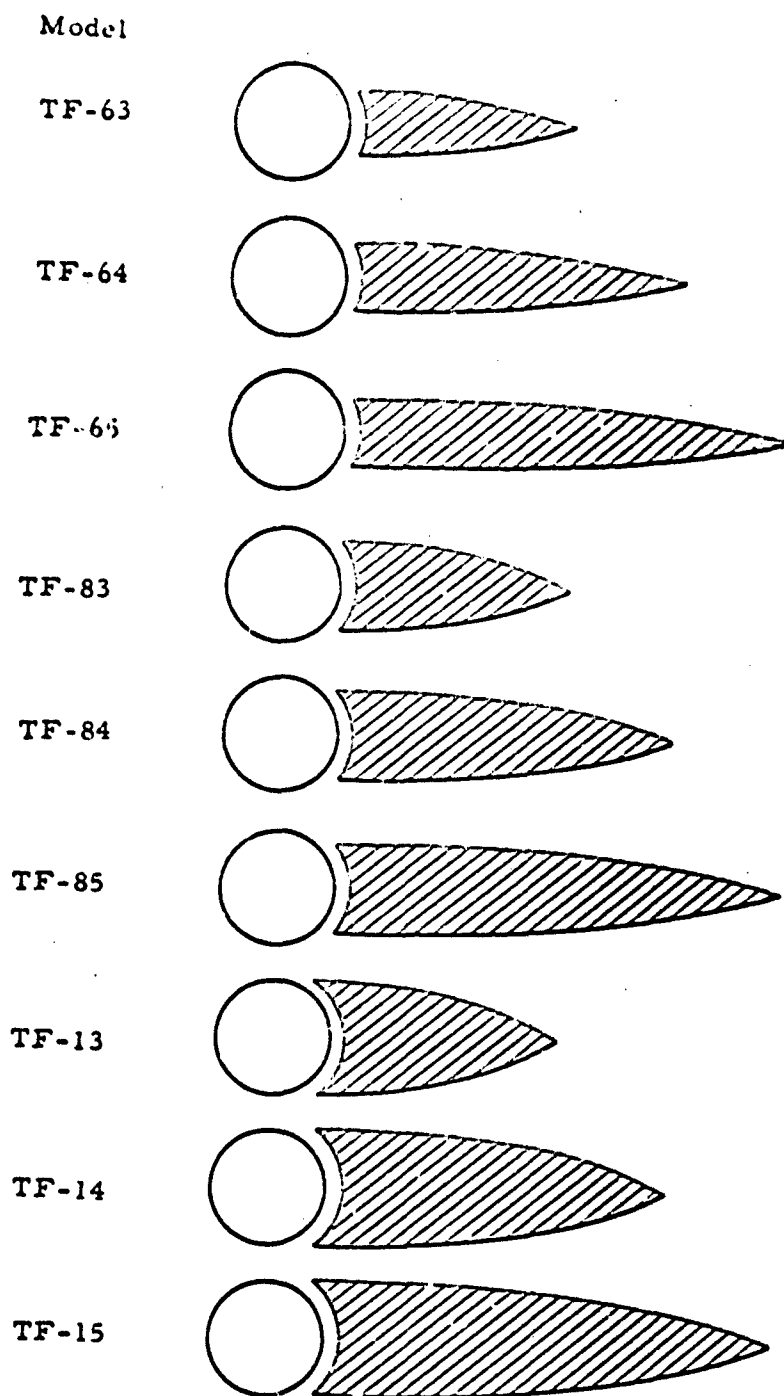


Figure 2 - Sketch of Section Shapes of Series A Test Models

Table 1 - Geometrical Parameters of Series A and B Shapes

Series A			Series B		
Designation	Thickness Ratio	Fineness Ratio	Designation	Thickness Ratio	Fineness Ratio
TF-63	0.6	3	B-1	0.6	2.875
TF-64	0.6	4	B-2	0.6	3.875
TF-65	0.6	5	B-3	0.6	4.875
TF-83	0.8	3	B-4	0.8	2.875
TF-84	0.8	4	B-5	0.8	3.875
TF-85	0.8	5	B-6	0.8	4.875
TF-13	1.0	3	B-7	1.0	2.875
TF-14	1.0	4	B-8	1.0	3.875
TF-15	1.0	5	B-9	1.0	4.875

DESCRIPTION OF MODELS

The models used for the tests are shown in Figure 3. The components of these models are the same as those used for the wind-tunnel tests but were assembled as shown in the figure for B-5.

The simulated cable is a 1.16-inch diameter model constructed by soldering 31 strands of 0.10-inch diameter copper rods to a 0.96-inch solid steel rod at a pitch angle of 75 degrees in a left hand lay. This simulated cable was modeled after an early tow cable used in the variable depth sonar program.

The fairing models are constructed of mahogany, are coated with a water-proofing sealer to prevent splitting, and are covered with several coats of paint to give them a smooth finish. Table 2 lists the physical characteristics of the Series B models. The wetted surface and chord length are computed with the models installed on the cable.

The length (span) of the models is 2 feet which is equivalent to the width of the test section of the two-dimensional dynamometer described later in this report.

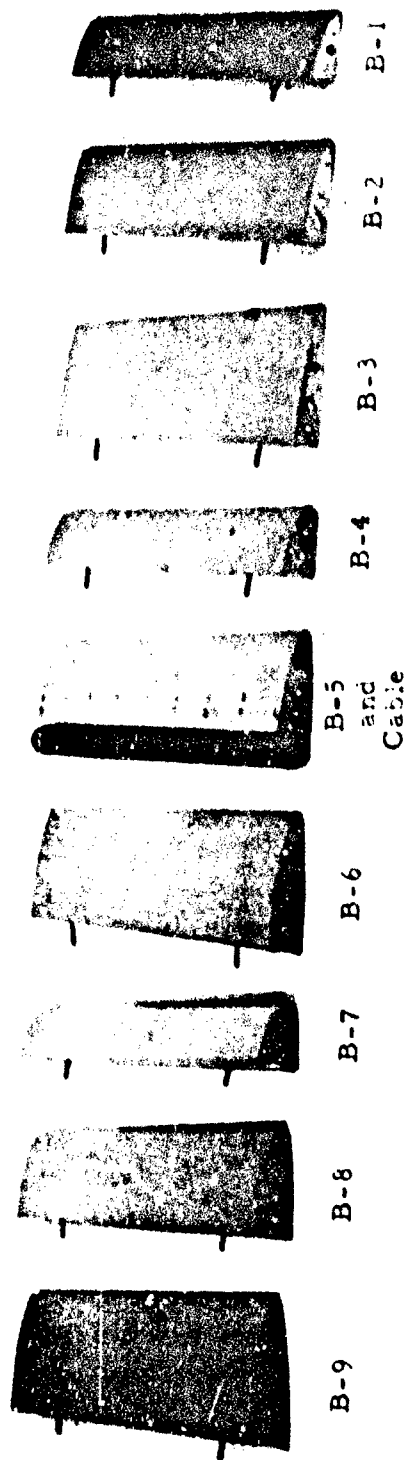


Figure 3 - Trailing Fairing Test Models

Table 2 - Physical Characteristics of Series B Models

Model	Wetted Surface Area, square feet	Chord Length, feet
B-1	1.26	0.28
B-2	1.63	0.38
B-3	2.00	0.47
B-4	1.26	0.28
B-5	1.63	0.38
B-6	2.00	0.47
B-7	1.26	0.28
B-8	1.63	0.38
B-9	2.00	0.47

TEST APPARATUS AND PROCEDURES

The drag on the fairing models was obtained using the two-dimensional fairing dynamometer shown in Figure 4. Figure 5 shows the gage arrangement in one of the wall balances of the dynamometer. Each wall balance is capable of measuring the lift and drag of the model. The output of the gages in the wall balances was amplified by TMB Type 211-2A control units and monitored with TMB Type T-1C digital strain indicators shown in Figure 6.

The fairing dynamometer assembly was designed to be installed on any of the Model Basin towing carriages. For this series of tests, the fairing dynamometer was attached to TMB Carriage No. 2. Figure 7 shows a schematic diagram of a typical test arrangement.

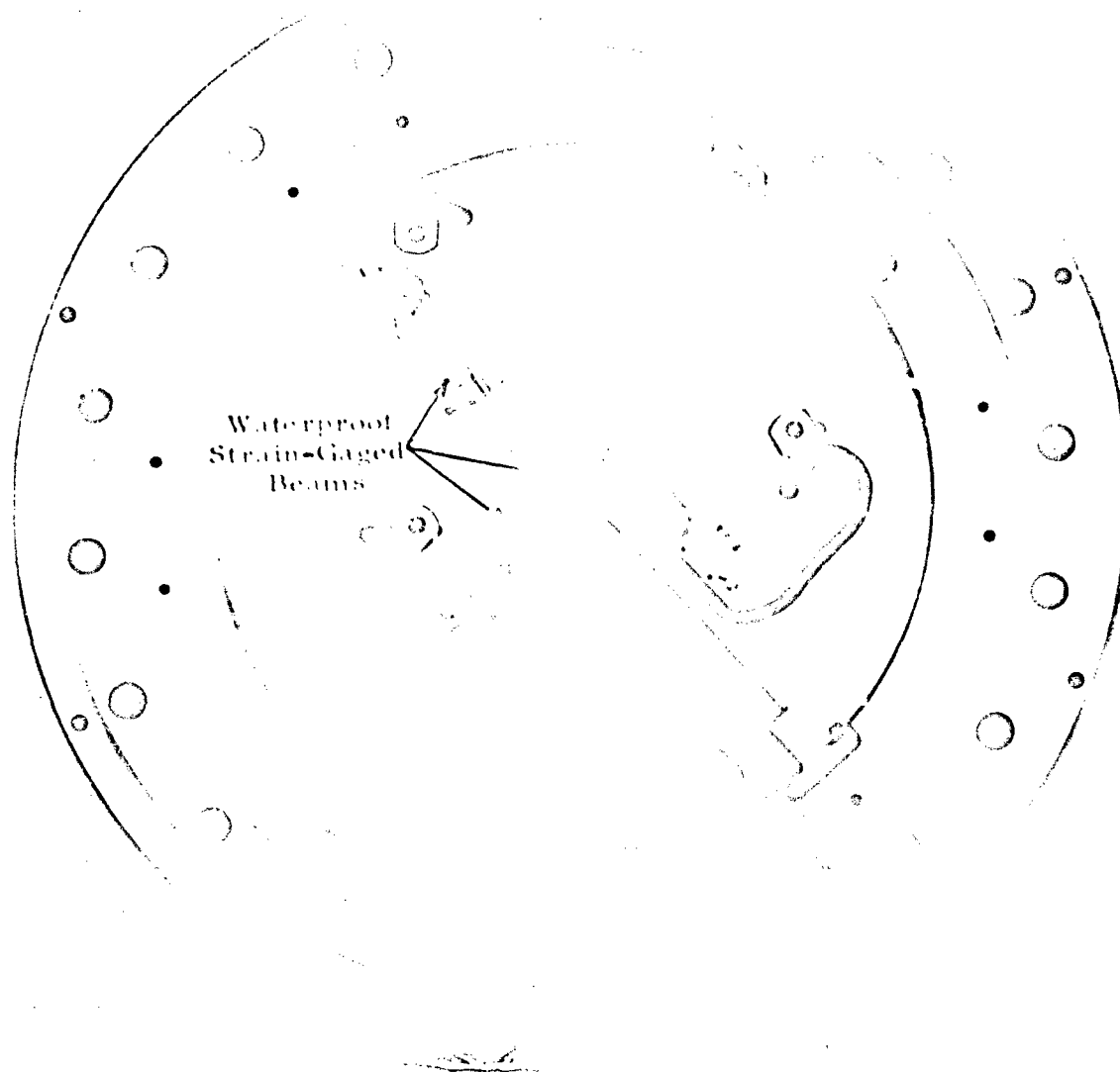
Prior to the formal test program, preliminary tests were conducted to determine the tare drag on the wall balance cover plates. In addition, a survey was made of the test section using a pitot-static tube to determine its velocity distribution.

Each of the Series B models was rigidly bolted to the wall-balance cover plate and the drag was measured at zero angle of attack for speeds from 0 to 12 knots. A separate test was made to determine the drag of the bare cable model for speeds from 0 to 12 knots.



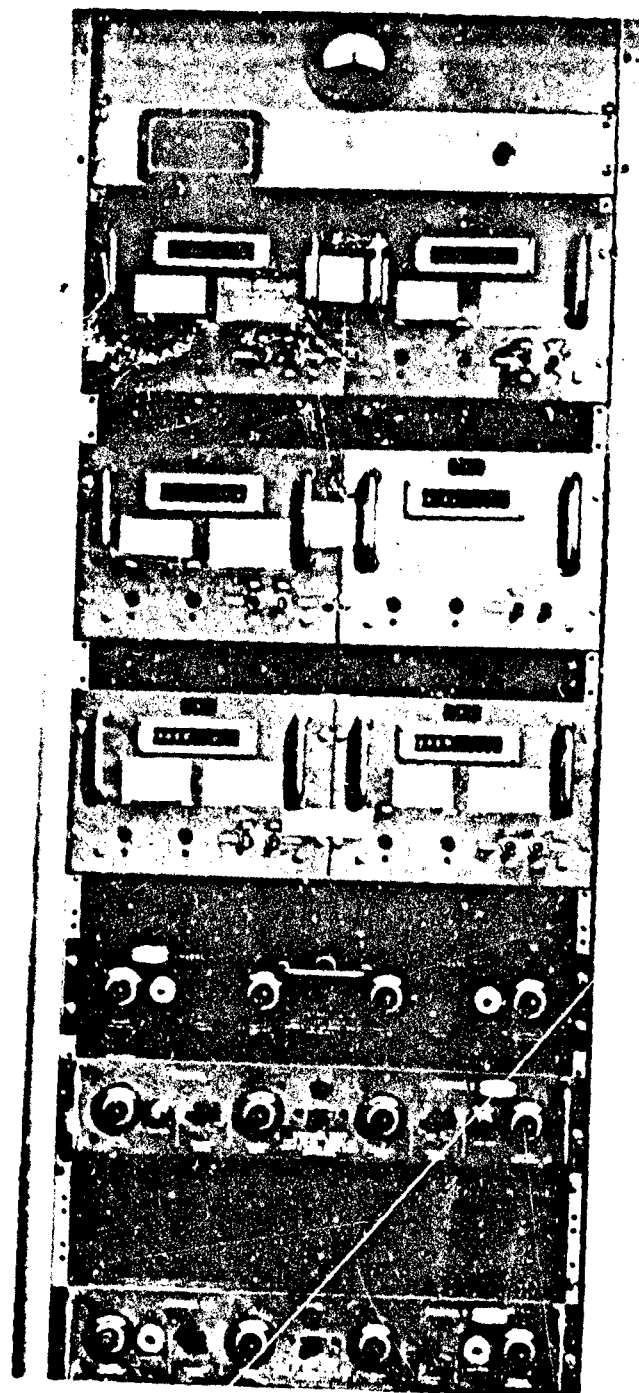
PSD 313574

Figure 4 - Two-Dimensional Fairing Dynamometer



PSD 311882

Figure 5 - Gage Arrangement



PSD 318618

Figure 6 - Instrumentation Arrangement

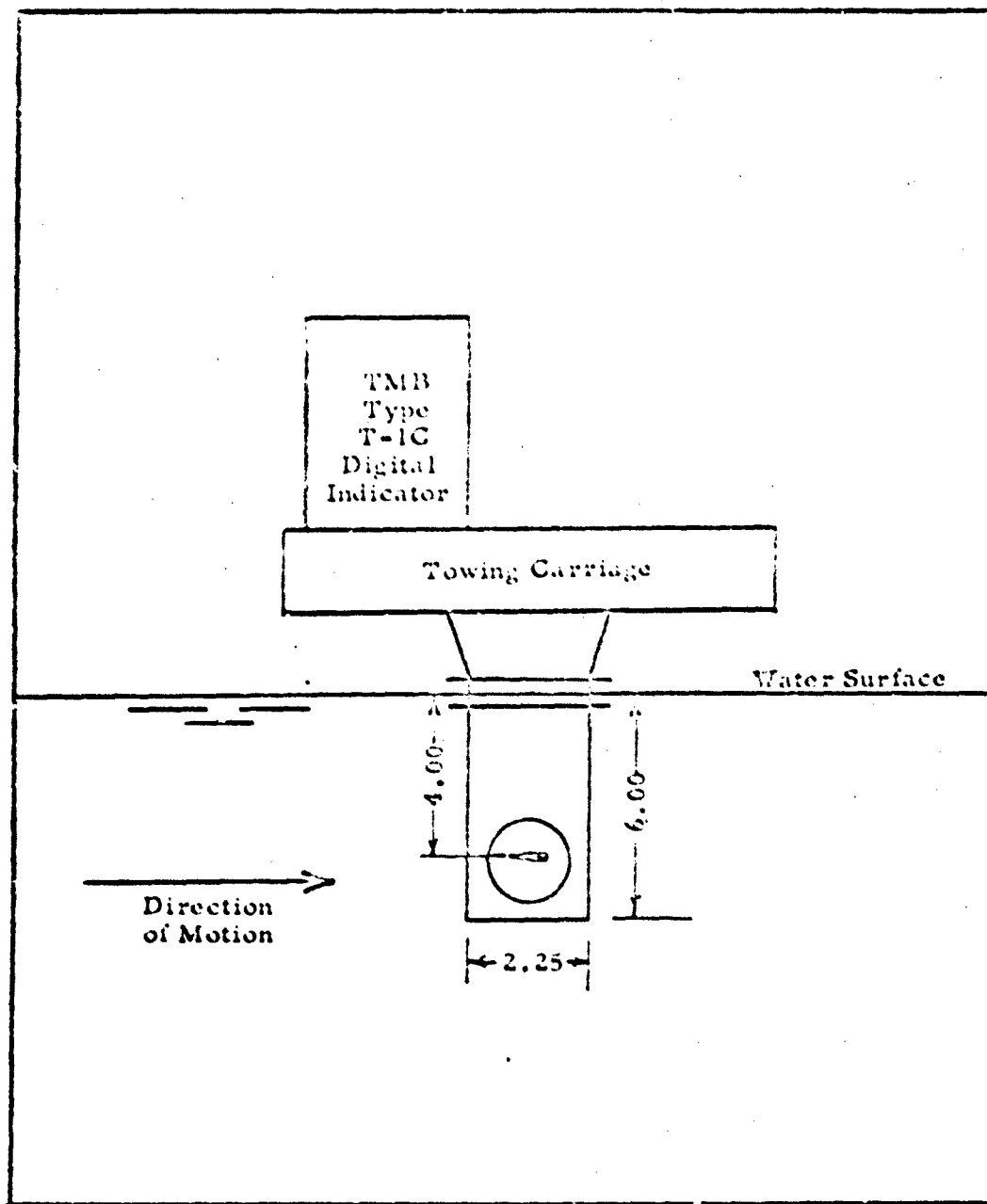


Figure 7 - Typical Test Arrangement
(All dimensions are in feet)

REDUCTION OF DATA

The results of the velocity survey indicated that over the range of speeds investigated, the velocity of the flow through the test section, except for that in immediate proximity to the wall-balance cover plate, was 2 percent lower than free stream. Consequently, the speed readings were reduced by 2 percent. Further, the drag readings were corrected for the tare drag of the cover plates. The drag coefficients C_D based on net drag, corrected speed, and projected frontal area A_f of the cable were computed for each of the fairing models and were plotted as a function of Reynolds number R which was based on cable diameter d as the characteristic length. The residual-resistance coefficient C_r was also calculated for each model by subtracting the frictional-resistance coefficient C_f (ATTC Line)⁴ from the total drag coefficient C_t .

RESULTS

Figures 8, 9, and 10 are plots of drag coefficients based on frontal area versus Reynold's number for fairing thickness ratios of 0.6, 0.8, and 1.0, respectively. Each figure is for a family of fineness ratios of 2.975, 3.875, and 4.875. In a separate analysis which is not shown in this report, it was found that curves of total drag coefficients versus Reynolds number paralleled the ATTC Line.

Figures 11 and 12 show the effect of varying the fineness ratio of the fairings while holding the thickness ratio constant on C_D and C_r , respectively. It can be seen from these figures that as the fineness ratio increases the drag decreases. This decrease is predominantly in the residual resistance, as shown by Figure 12.

Figures 13 and 14 show the effect on the drag coefficient and residual-resistance coefficient, respectively, of varying the thickness ratio while holding the fineness ratio constant. Figure 13 shows that increasing thickness ratio (up to a value of 1.0) tends to decrease the drag. Here again, the decrease is predominantly in residual resistance, as shown by Figure 14.

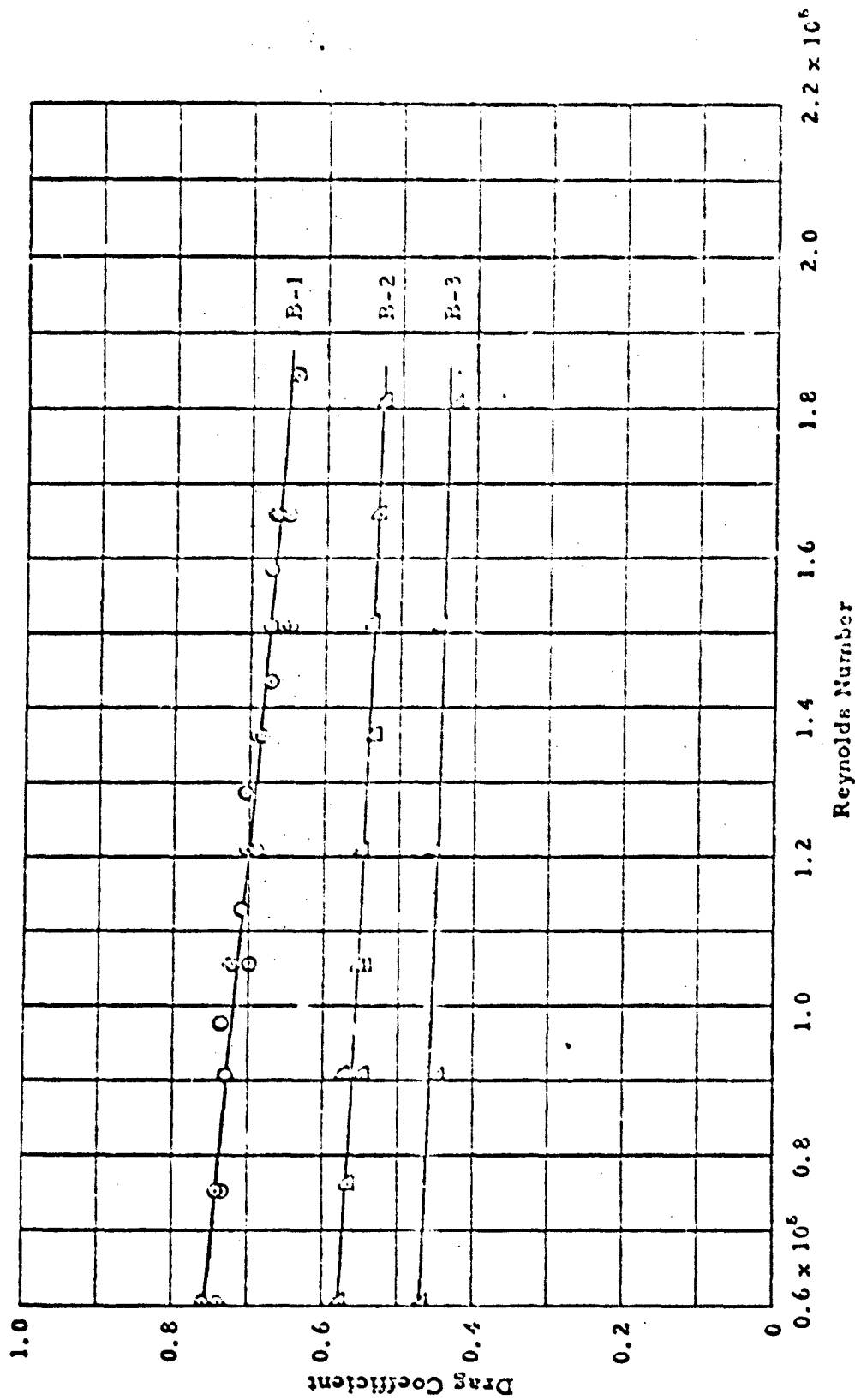


Figure 8 - Drag Coefficient as a Function of Reynolds Number for a Thickness Ratio of 0.6
(Drag coefficient based on frontal area; Reynolds number based on cable diameter)

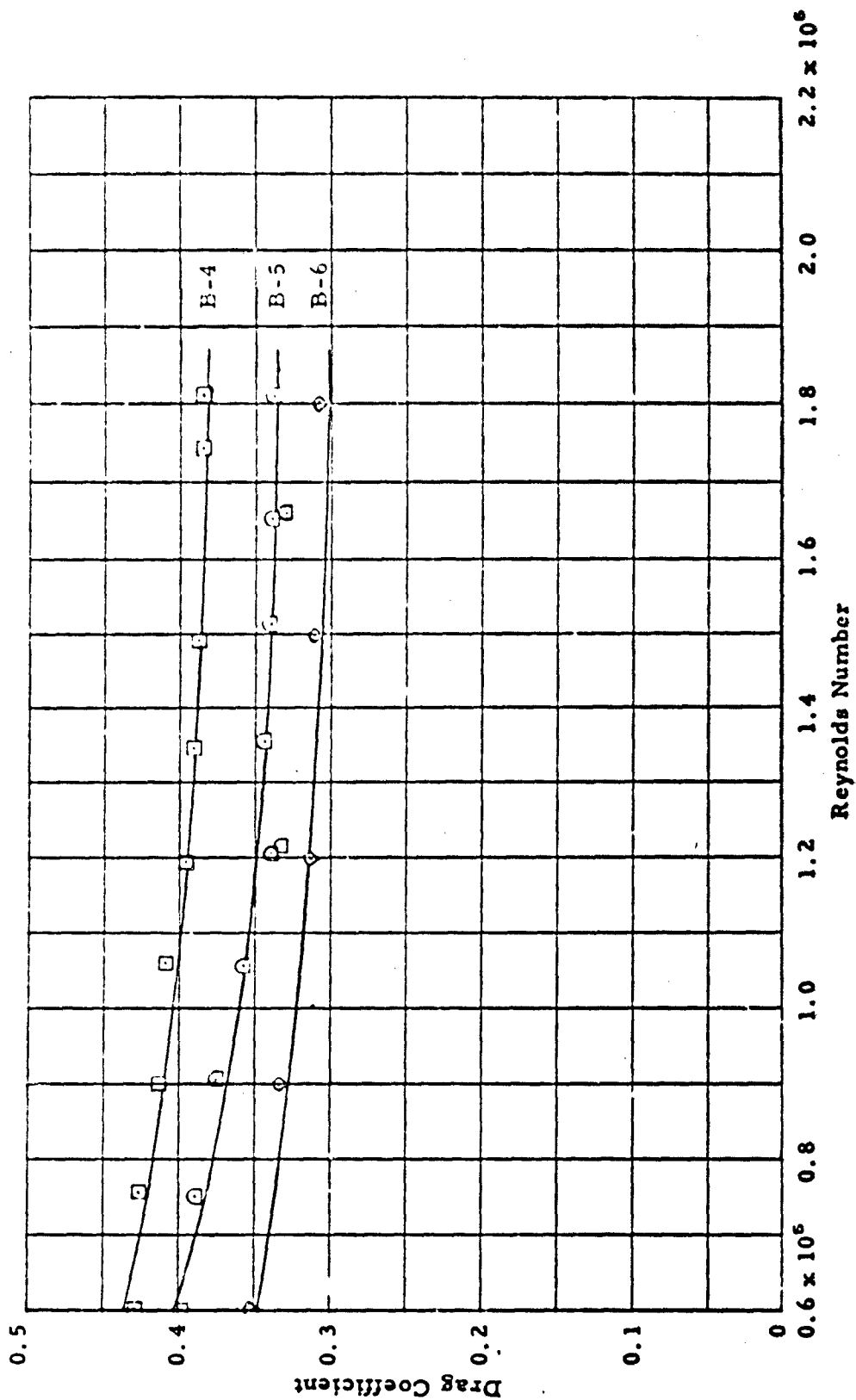


Figure 9 - Drag Coefficient as a Function of Reynolds Number for a Thickness Ratio of 0.8
(Drag coefficient based on frontal area; Reynolds number based on cable diameter)

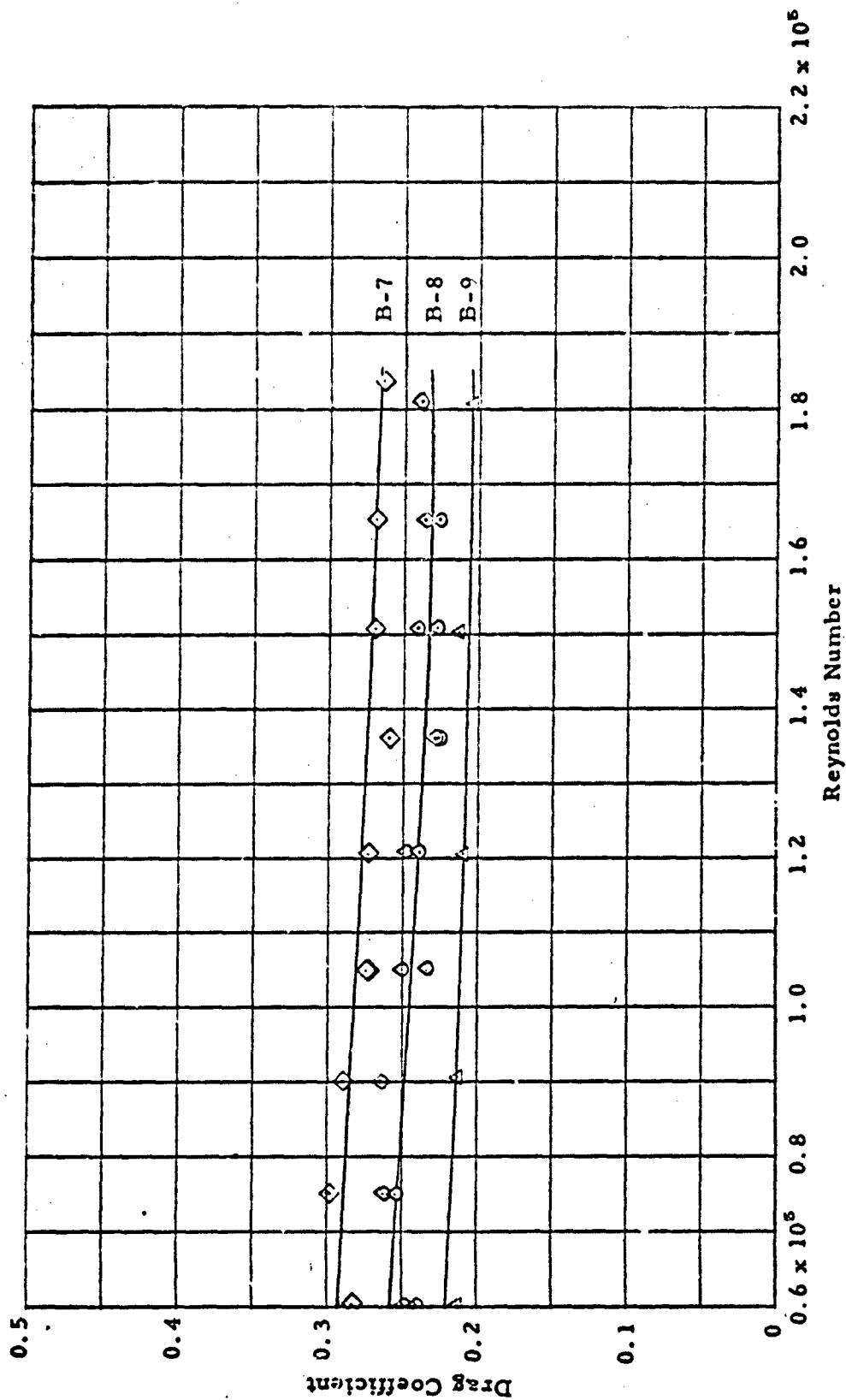


Figure 10 - Drag Coefficient as a Function of Reynolds Number for a Thickness Ratio of 1.0
(Drag coefficient based on frontal area; Reynolds number based on cable diameter)

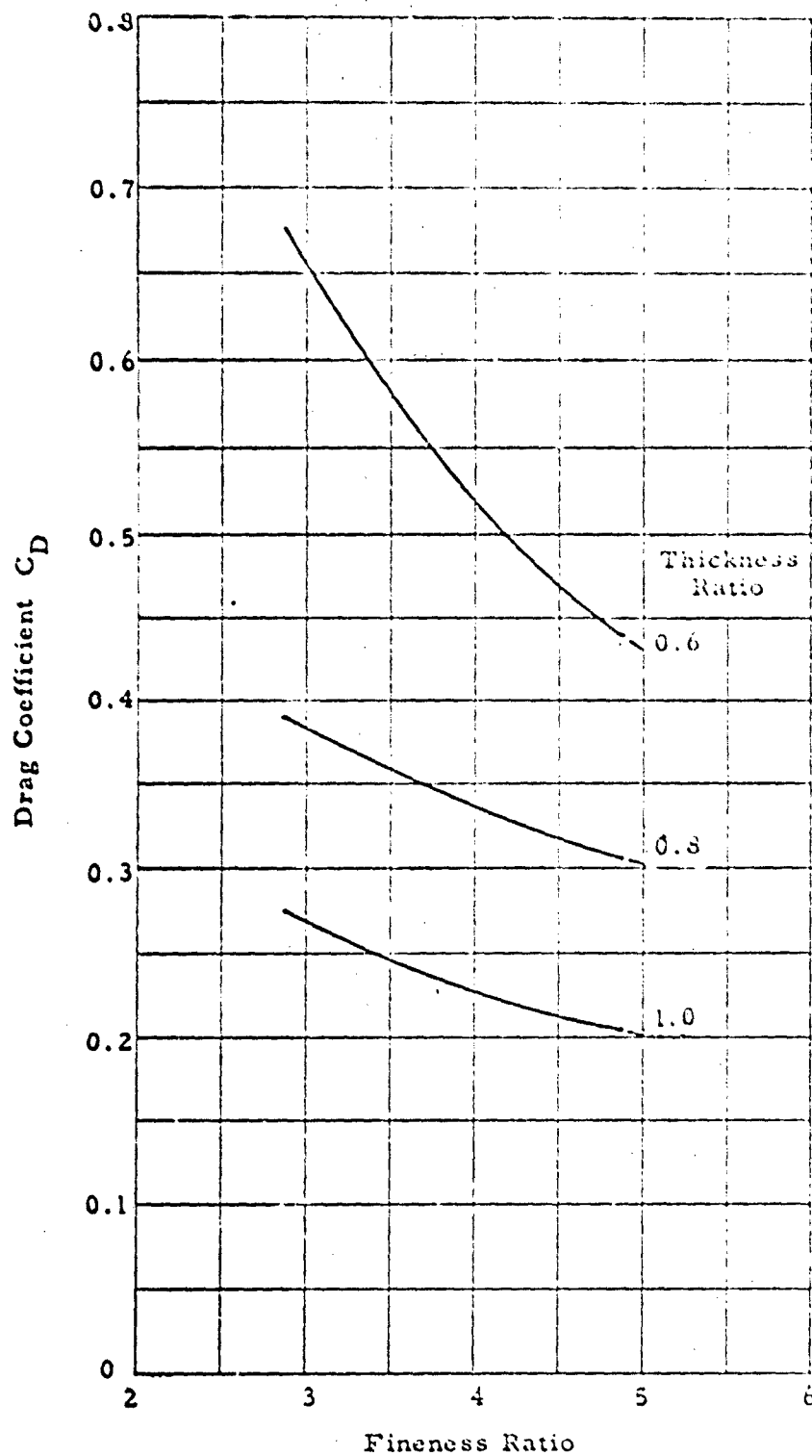


Figure 11- Effect of Fineness Ratio on Drag Coefficient
(Reynolds Number - 1.5×10^5)

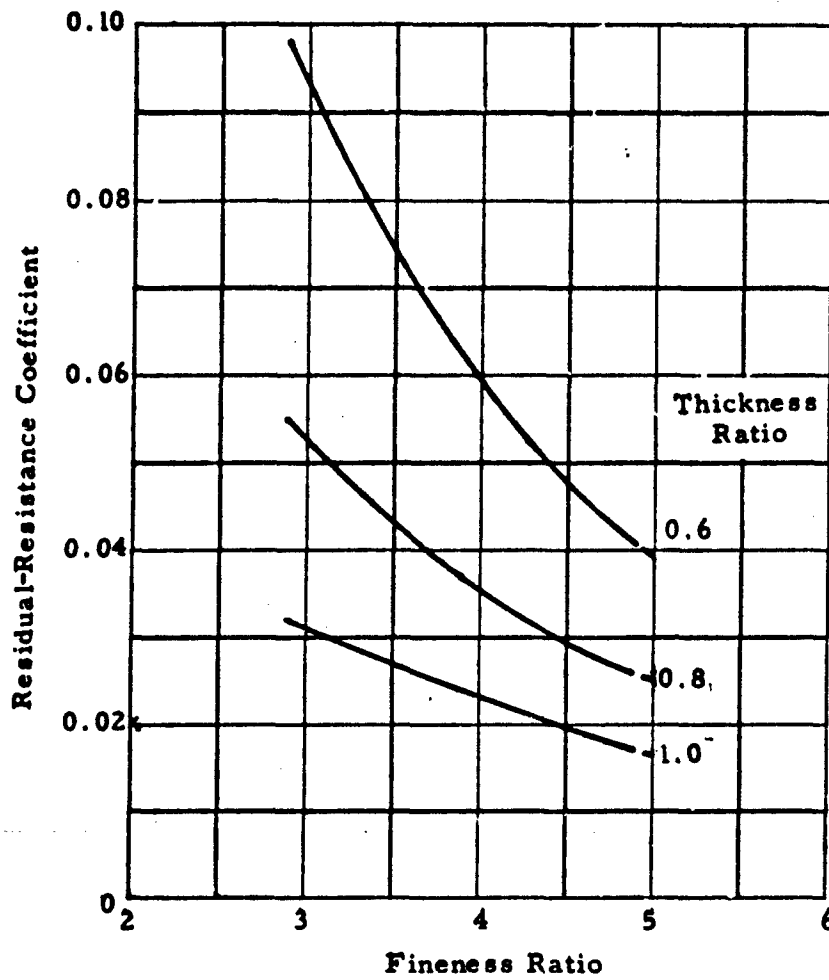


Figure 12 - Effect of Fineness Ratio on Residual-Resistance Coefficient

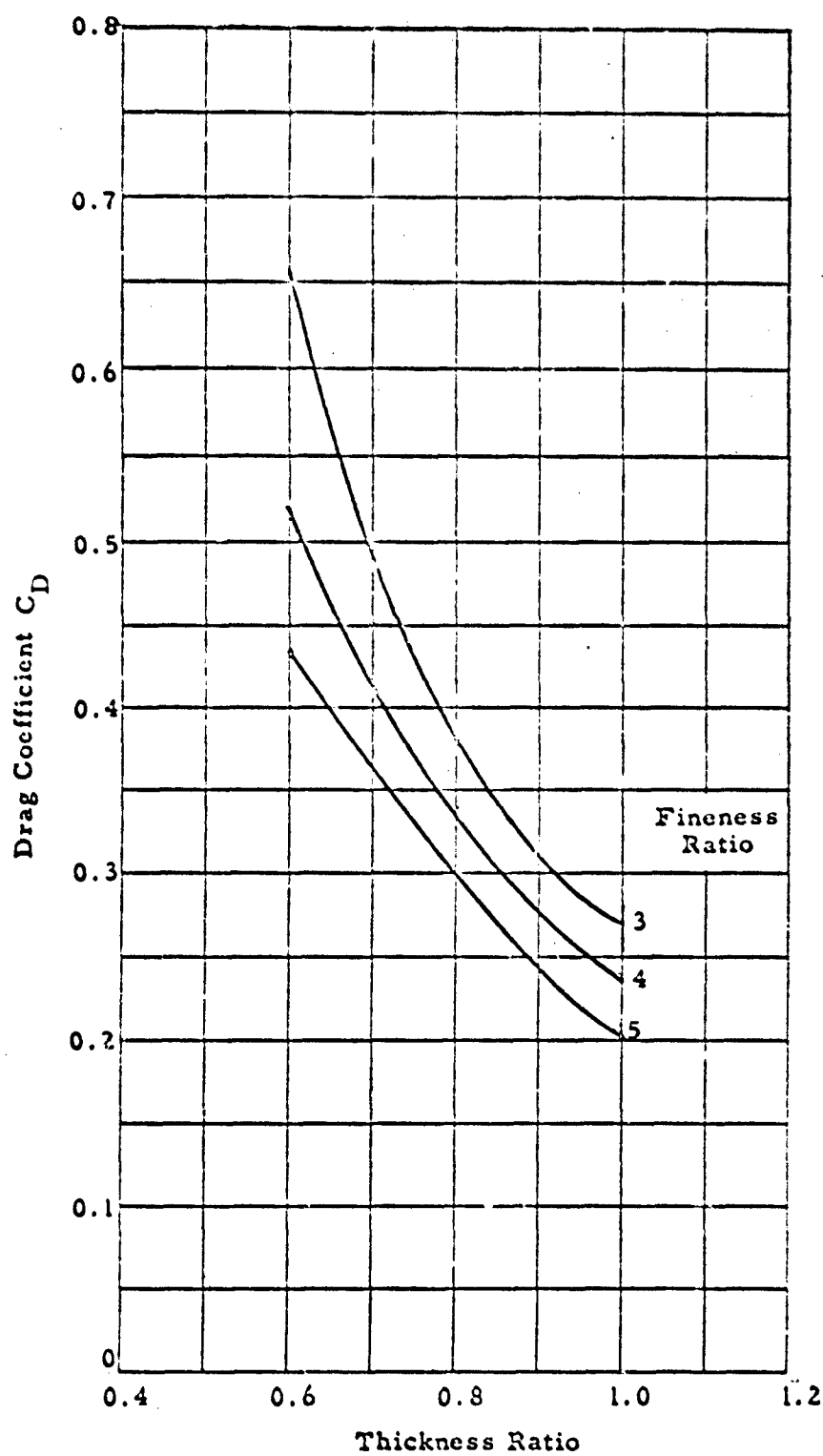


Figure 13 - Effect of Thickness Ratio on Drag Coefficient
(Reynolds Number - 1.5×10^5)

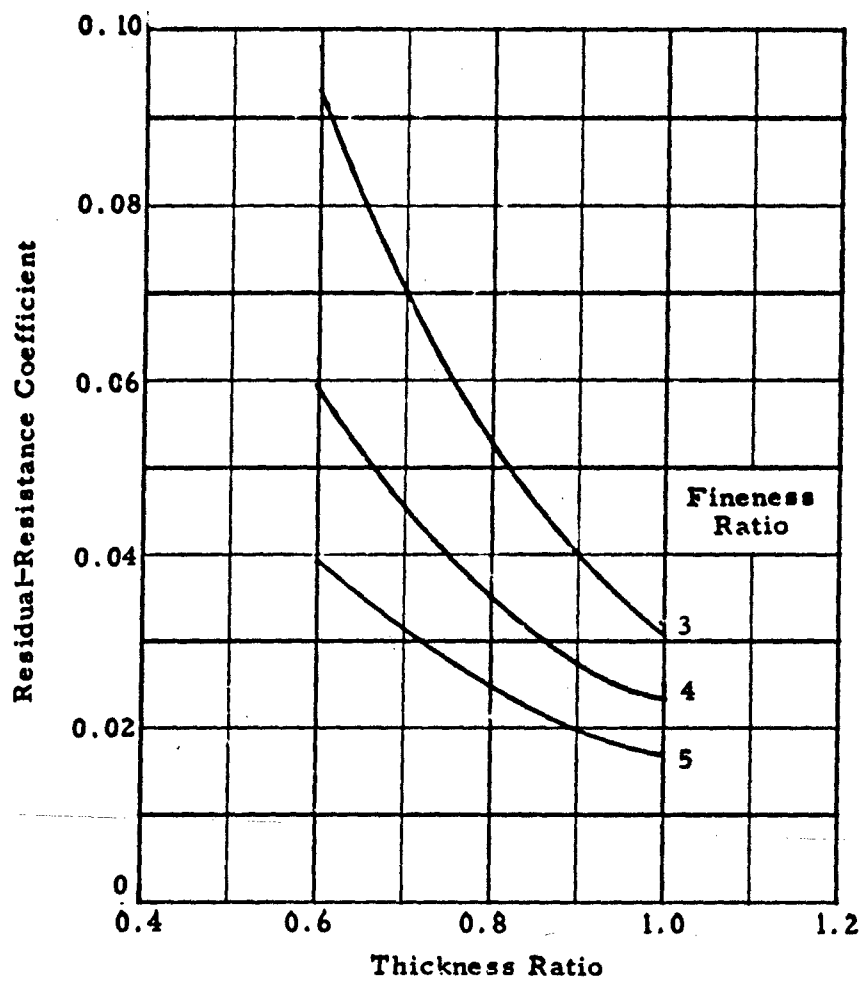


Figure 14 - Effect of Thickness Ratio on Residual-Resistance Coefficient

The drag coefficient C_D of the bare-cable model was nearly constant at a value of 0.985 over the speed range tested. This is a much lower value than commonly used for bare cables in calculations of cable configurations and can be attributed to the fact that the test cable was rigid and was restrained from vibration by being held at both ends. In calculations, the Model Basin usually uses a drag coefficient of 1.5 for bare cable based on an unpublished correlation of predicted values and full-scale experimental data. Nevertheless, all of the fairings in the series produced a substantial reduction in the drag of the bare cable.

CONCLUSIONS

Based on the results of drag tests on a systematic series of trailing-type cable fairings, the following conclusions are drawn:

1. The drag decreases with increasing fineness ratio in the range of ratios from 2.875 to 4.875. This is due primarily to a reduction in residual resistance.

2. The drag decreases with increasing thickness ratio in the range of ratios from 0.6 to 1.0. This is also due to a reduction in residual resistance.

3. All of the fairings used in the series produce a substantial reduction in the drag coefficient of a bare cable. The lowest drag coefficient ($C_D = 0.2$) was obtained with the model having a fineness ratio of 4.875 and a thickness ratio of 1.0. The drag coefficient of the rigid simulated cable used in the experiments is 0.985, but a more realistic figure for a bare cable used at sea is a drag coefficient of 1.5.

4. Since the total-drag coefficients of each model paralleled the ATTC Line, the residual-drag coefficient of each model is, for all practical purposes, independent of Reynolds number. Thus, the total-drag coefficient C_t can be determined for any Reynolds number beyond transition by adding the frictional-resistance coefficient C_f for that Reynolds number to the particular C_r for the fairing shape of interest.

ACKNOWLEDGMENTS

The authors wish to express their gratitude to the following who contributed to the completion of this project. The initial work of deriving the equations of the trailing-fairing shape by Dr. L. F. Whicker is greatly appreciated. Thanks are also due to Mr. John Bankovskis and Mr. C. O. Walton who aided in conducting the velocity survey and the actual testing of the fairing models.

REFERENCES

1. Velebnay, R. L., "Wind-Tunnel Tests of Two-Dimensional Faired Cables, Part II - Additional Tests at Higher Reynolds Numbers (U)," David Taylor Model Basin Report C-981 Aero Report 921 (August 1958) **CONFIDENTIAL.**
2. Ziegler, N. G., "Wind-Tunnel Tests of Two-Dimensional Cable Fairings," David Taylor Model Basin Report 1284 Aero Report 952 (November 1958).
3. Ziegler, N. G., "Wind-Tunnel Tests of Two-Dimensional Cable Fairings, Addendum-Results of Retests of Towed Cable Fairings," David Taylor Model Basin Report 1284 Aero Report 952 (May 1962).
4. Gertler, M., "The Prediction of the Effective Horsepower of Ships by Methods in Use at the David Taylor Model Basin," David Taylor Model Basin Report 576 (December 1947).